J Neurophysiol 119: 21–32, 2018.
First published September 20, 2017; doi:10.1152/jn.00519.2017.

RESEARCH ARTICLE | *Control of Coordinated Movements*

Cue-induced changes in the stability of finger force-production tasks revealed by the uncontrolled manifold analysis

Mitchell Tillman and Satyajit Ambike
Department of Health and Kinesiology, Purdue University, West Lafayette, Indiana

Submitted 10 July 2017; accepted in final form 16 September 2017

Tillman M, Ambike S. Cue-induced changes in the stability of finger force-production tasks revealed by the uncontrolled manifold analysis. *J Neurophysiol* 119: 21–32, 2018. First published September 20, 2017; doi:10.1152/jn.00519.2017.—A motor system configured to maximize the stability of its current state cannot dexterously transition between states. Yet, we routinely resolve the stability-dexterity conflict and rapidly change our current behavior without allowing it to become unstable before the desired transition. The phenomenon called anticipatory synergy adjustment (ASA) partly describes how the central nervous system handles this conflict. ASA is a continuous decrease in the stability of the current motor state beginning 150–400 ms before a rapid state transition accomplished using redundant sets of motor inputs (more input variables than task-specific output variables). So far, ASAs have been observed only when the timing of the upcoming transition is known. We utilized a multifinger, isometric force-production task to demonstrate that compared with a condition where no state transition is expected, the stability of the current state is lower by ~12% when a participant is cued to make a transition, even when the nature and timing of that transition are unknown. This result (stage 1 ASA) is distinct from its traditional version (stage 2 ASA), and it describes early destabilization that occurs solely in response to the expectation to move. Stage 2 ASA occurs later, only if the timing of the transition is known sufficiently in advance. Stage 1 ASA lasts much longer (~1.5 s) and may scale in response to the perceived difficulty of the upcoming task. Therefore, this work reveals a much refined view of the processes that underlie the resolution of the stability-dexterity conflict.

NEW & NOTEWORTHY We compared the stability of multifinger, isometric force-production tasks for trials in which force changes of unknown direction and timing were expected with trials in which there was no expectation of any force change. Mere expectation of a change caused the stability of the current motor state to drop. This novel result provides a much refined view of the processes that facilitate dexterous switching between motor states.

uncontrolled manifold; manual dexterity; finger force; redundancy; anticipatory synergy adjustment

INTRODUCTION

Maintaining stability of a motor action is a critical attribute of a healthy motor system. Stability is the ability to maintain the current static or dynamic motor state by dissipating the effects of neuromuscular and environmental disturbances. There is converging evidence suggesting that the central nervous system (CNS) ensures stability by exploiting the redundancy in the motor apparatus, i.e., the structural feature that there are more input variables than output variables associated with most motor tasks (Bernstein 1967). Redundant systems afford solution sets (or spaces) rather than unique solutions for a task. Evidently, the CNS dissipates internal or external perturbations in part by channeling its effects into the abundant solution space, thereby mitigating their influence on the output variables (Dingwell et al. 2010; Latash 2012; Mattos et al. 2011; Müller and Sternad 2009; Scholz et al. 2007; Schoner 1995; Todorov and Jordan 2002). Motor redundancy, therefore, facilitates the stability of motor action.

The notion of a synergy is one theoretical framework that formalized this idea. It is defined as a neural organization that ensures covariation of the input variables such that a value or a time profile of an important output (task) variable is stabilized (Latash 2008). Synergies, quantified using the uncontrolled manifold (UCM) method (Scholz and Schöner 1999), have been observed in several behaviors performed by healthy and impaired human participants (reviewed in Latash 2008; Latash et al. 2007). The UCM analysis yields a synergy index (ΔV), which reflects the stability conceived as the reproducibility of task variables or their time profiles across multiple trials (see METHODS).

However, several researchers have stressed that maximizing stability is not desirable when adaptable behavior is required to achieve task goals (Hasan 2005; Latash and Huang 2015; Riccio 1993; Riccio and Stoffregen 1988; Riley and Turvey 2002). Dexterity is the ability to rapidly transition between motor states in response to changing task demands (Bernstein 1996), and it is antithetical to stability (Santisteban et al. 2016). Over the last decade, the notion of anticipatory synergy adjustment (ASA) has emerged, which begins to capture the CNS's strategy for managing this dexterity-stability conflict. A drop in the synergy index is observed beginning 150–400 ms before any changes in the task-specific output variables are observed. This drop in ΔV is called ASA, and it describes the reduction in stability as the system prepares to change the output variables. ASA has been observed in manual tasks (Kim et al. 2006; Olafsdottir et al. 2005; Park et al. 2012; Shim et al. 2006; Togo and Imamizu 2016) and postural tasks involving quick shifts of the center of pressure (Klous et al. 2011; Krishnan et al. 2011; Piscitelli et al. 2017; Wang et al. 2006).

Address for reprint requests and other correspondence: S. Ambike, Dept. of Health and Kinesiology, 800 West Stadium Ave., Purdue Univ., West Lafayette, IN 47907 (e-mail: sambike@purdue.edu).

Note that ASA measurements with existing techniques require that a state change occurs. Because ASA appears immediately before the change, it could be viewed as a part of the execution of that motor action. In this study, we aimed to isolate the synergy adjustment associated with mere anticipation, divorced from subsequent state change. If such adjustment exists, it would qualify as motor planning rather than execution. The task we employ is essentially a choice reaction-time (CRT) task in which an initial warning cue is provided, followed by a blank interval (foreperiod), followed by a reaction signal that identifies, from a predefined set, the particular action that the participant must execute as fast as possible. It is well known that performance in the CRT task changes (faster response time, reduced errors) when the participant is cued by the warning signal, even when the cue provides no information about the nature of the upcoming motor action (Brunia 1993; Goodman and Kelso 1980; Jahanshahi et al. 1992). Presumably, a generalized motor preparation, or planning, that is somehow common to all the possible upcoming actions occurs during the foreperiod and leads to these improvements in dexterous task switching (Brunia 1993; Jahanshahi et al. 1992; Niemi and Naatanen 1981; Wu et al. 2015). It is plausible that ASA represents this generalized planning for actions involving redundant input variable sets, and as such, they would be interpreted as improvements in dexterity. However, to make this claim, a change in ΔV must be observed across a cue condition: ΔV during a foreperiod of a reaction-time task must be smaller than ΔV when no action is expected. This comparison has not been made. In all previous studies, ASA was measured as the drop in ΔV at the instant when the task variable first changes relative to a baseline ΔV measured earlier (e.g., 500 ms before the task variable changes; cf. Latash and Huang 2015) for trials in which a rapid action is always expected.

Furthermore, in existing work, ASAs appear mostly when the participant knows the timing of the upcoming motor action. ASAs appear in self-paced manual force-production tasks when both the timing and the direction of the impending action are known to the participant (Olafsdottir et al. 2005; Zhou et al. 2013) and in postural tasks involving perturbations of unknown directions administered by the participants themselves (Piscitelli et al. 2017). In contrast, ASA disappears in cued simple reaction-time tasks when only the timing of the action is unknown (Olafsdottir et al. 2005; Shim et al. 2006; Zhou et al. 2013). Nevertheless, it is plausible that ΔV reduces across a cue condition in reaction-time tasks, despite the uncertainty in the timing.

Finally, it is plausible that ASA scales with respect to the perceived difficulty of the task. This is consistent with the view that the CNS utilizes probabilistic models of the task to optimize performance (Körding and Wolpert 2004; Wolpert and Landy 2012). Therefore, if such a model generates expectations of faster required responses or larger response sets, the CNS may reduce ΔV more during the foreperiod.

The present study explored these possibilities using an isometric finger force-production task in healthy, young adults. ASA has been observed for such tasks in diverse populations, including healthy young (Olafsdottir et al. 2005; Shim et al. 2006; Zhou et al. 2013) and older adults (Olafsdottir et al. 2007, 2008) and persons with neurological deficits (Jo et al. 2017; Park et al. 2012). The objectives of the present study were to establish if *1*) the stability of the current manual state is diminished by cuing the participant for quick motor action, *2*) the cue effect is sensitive to the uncertainty in the timing of the upcoming action, and *3*) the cue effect scales with the degree of difficulty of the expected action. Participants used the four fingers of the dominant hand to produce a single output force computed as the sum of the individual finger forces. They produced the same steady total force as part of three experimental tasks. In the stable task, they expected to maintain the total force. In the slow dexterous task, they expected to either increase or decrease their total force at an unknown time in the near future. The fast dexterous task was similar to the slow dexterous task, except that participants expected a faster force change. The synergy index for all three tasks was computed. For the dexterous tasks, the period when ΔV is computed is analogous to the foreperiod, the blank interval between the presentation of the warning cue and the response cue, in traditional CRT paradigms (Niemi and Naatanen 1981).

Two specific hypotheses were tested. The first hypothesis was that the synergy index in the stable task (participant not cued for quick action) would be greater than that for the slow and fast dexterous tasks (participant cued for action) despite uncertainty in the timing of the upcoming action. The second hypothesis was that the synergy index would drop more for the fast dexterous task compared with the slow dexterous task.

METHODS

Participants

Twenty-five participants volunteered to participate in the study [19 women; age, 20.4 ± 2.6 yr; weight, 65.4 ± 13.3 kg; height, 1.68 ± 0.08 m (means ± SD)]. Two participants were left-hand dominant and 23 right-hand dominant by self-report, and no participant had any history of neurological issues or musculoskeletal discomfort or injury in the upper arm. All participants provided written informed consent in accordance with the procedures, which were approved by the Institutional Review Board of Purdue University.

Equipment and Procedures

Participants sat comfortably in a chair with both forearms resting on top of a table. They extended all the fingers of their dominant hand and placed the fleshy part of the distal phalanx facing downward on four separate force sensors (Nano 17; ATI Industrial Automation, Garner, NC) as shown in Fig. 1*A*. The diameter of the sensors was 17 mm, and the distance between sensors was 30 mm. The signals from the transducers were collected by The MotionMonitor software (Innovative Sports Training) and digitized at 1,000 Hz. The sensor readings were zeroed with the fingers resting on the sensor and with the hand relaxed so that the weight of the fingers was excluded from the sensor readings. For all experimental trials, the sum of the vertical forces ($F_T = \Sigma F_i$, where i = index, middle, ring, and little finger) was presented as feedback to the participant as a cross on a 19-in. computer screen placed ~0.8 m in front of the participant (Fig. 1*B*). The cross moved upward if the participant increased F_T, and vice versa.

The participants first performed maximum voluntary contraction (MVC) trials in which they pressed on the sensor using all four fingers as hard as possible, achieved maximal force level within 6 s, and relaxed immediately after reaching maximal force. They performed three consecutive MVC trials with 1-min rest intervals, and the average of the three F_T maxima was used to design the experimental tasks. For the next task, two square icons, the same size as the cross, representing 5% and 15% of the participant's MVC were presented on

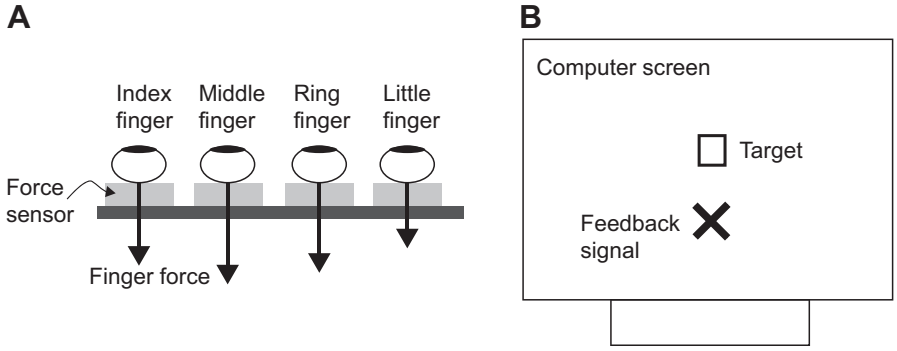

Fig. 1. *A*: experimental setup. Participants placed the 4 fingers of the dominant hand on 4 force sensors and pressed on them. *B*: feedback. A computer screen placed in front of the participant displayed the total finger force as a cross. The cross moved upward when the total finger force increased, and vice versa. Total force target(s) was displayed as square icon(s).

the screen as the targets (Fig. 2*A*). Participants oscillated their total finger force between the two targets as fast as possible, and the maximum force rate was recorded. These values were used to ensure that the tracking tasks described below required force-production rates that were significantly lower than their maximal abilities. This rapid force variation task lasted 7 s, and the participants repeated the task three times with 30-s breaks between trials.

Next, participants performed three experimental tasks. For the stable task, participants modulated F_T to match a target square icon representing 10% MVC for 7 s. They were informed that the target would be stationary during the trial. For the second and the third tasks, called slow dexterous and fast dexterous tasks, respectively, participants modulated F_T and tracked the square target as it moved in the vertical direction. They were aware that the target would move but unaware of its trajectory. A typical dexterous task trajectory, depicted in Fig. 2*B*, consisted of linear ramp segments connecting steady force values and lasted 30 s. The slopes of the ramps and the magnitudes and durations of the steady target forces varied within and across the trajectories. The trajectories were bounded between 5% and 15% MVC, and they included force rates that were well within the participants' maximal abilities (estimated from pilot data). Each trajectory contained one portion of 10% MVC, matching the target for the stable task. The location of this portion varied across tasks, and its duration varied between 4.04 and 5.5 s. The variable duration of this portion introduced timing uncertainty in the upcoming action. We emphasize that the participants were unaware of the specifics of the task design. Eight different target force trajectories were composed for the slow and fast dexterous tasks, each.

The target profiles for the slow and fast dexterous tasks produced the same impulse on average [slow dexterous profiles: 293.5 ± 18.88%MVC·s; fast dexterous profiles: 293.5 ± 7.16%MVC·s; $t_{(7)} = 0.001$; $P = 0.999$]. The key difference between the two tasks was that the target moved much faster for the fast dexterous task. This designed difference in the target profiles made the fast dexterous task more difficult, and during the constant 10% MVC portion of these trials, the participants expect to execute a faster F_T change in the near future. Across the 8 target profiles for the fast dexterous task, the maximum absolute force rate was 102.58 ± 92.1%MVC/s, the highest absolute force rate was 297.95%MVC/s, the mean force rate was 2.57 ± 0.37%MVC/s, and the power concentrated within the 0- to 2-Hz band was 65.32 ± 5.14%. In contrast, across the 8 target profiles for the slow dexterous task, the maximum absolute force rate was 20.56 ± 10.7%MVC/s, the highest absolute force rate was 38.37%MVC/s, the mean force rate was 1.75 ± 0.24%MVC/s, and the power concentrated within the 0- to 2-Hz frequency band was 81.75 ± 6.08%.

Each of the 8 trajectories was presented twice to obtain a set of 16 trials for the slow and the fast dexterous tasks. Similarly, the stable task was repeated 16 times. The number of trials for each task was based on the typical number of trials used in most UCM analyses of finger forces (Olafsdottir et al. 2005; Zhou et al. 2013). The task types were block randomized across participants, and the trial sequences were randomized within each block for the slow and the fast dexterous tasks.

To gain familiarity with the fast and slow dexterous tasks, participants performed ten 15-s trials in which they tracked a moving target before starting the experimental trials. The trajectories used for these practice trials were different from those used for the experimental trials.

To limit fatigue, a rest break was given between all repetitions. Two-minute breaks were given after each kind of task was performed: MVC trials, rapid force oscillation trials, practice trials, and the three kinds of experimental trials. Breaks of 30 s were given after each trial in the practice set, 15-s breaks were enforced after each trial of the stable task, and 30-s breaks were given after each trial of the slow and fast dexterous tasks. Participants were instructed to ask for additional rest if they felt fatigued at any point in the experiment. The entire experiment took ~90 min, and none of the participants reported any fatigue during this study.

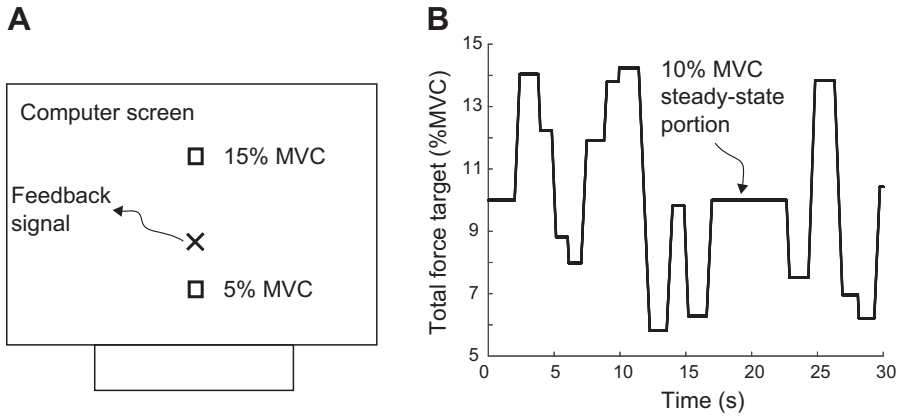

Fig. 2. *A*: feedback for the rapid force oscillation tasks. Two square targets at 5% and 15% MVC were displayed on the screen, along with the participant's current total force. *B*: typical total force target trajectory for the slow and fast dexterous tasks. The trajectories were composed of linear ramps connecting varying durations and magnitudes of constant force. Each trajectory contained one portion of 10% MVC that lasted at least 4 s.

Data Analysis

MATLAB programs were written for data analysis. All data were low-pass filtered at a cutoff frequency of 10 Hz using a fourth-order, zero-lag Butterworth filter. The performance of the slow and the fast dexterous tasks was quantified using cross-correlation analysis between the generated and the target total force traces. The last 4 s of the 16 trials for the stable task were selected (Fig. 3*A*) for the UCM analysis, described below. For the slow and fast dexterous trials, the 16 responses were time-aligned with respect to the start of the extended 10% MVC portion (lasting over 4 s) separately (Fig. 3*B*). The first 4 s of the responses during this portion were isolated for the UCM analysis. Note that the local task demands for the stable and the dexterous tasks are identical (F_T = 10% MVC) for the selected responses. Furthermore, because the period of 10% MVC lasted at least 4.04 s, we analyze the behavior before the square target begins to move, and thus study the motor planning associated with the impending state change rather than the execution of that state change.

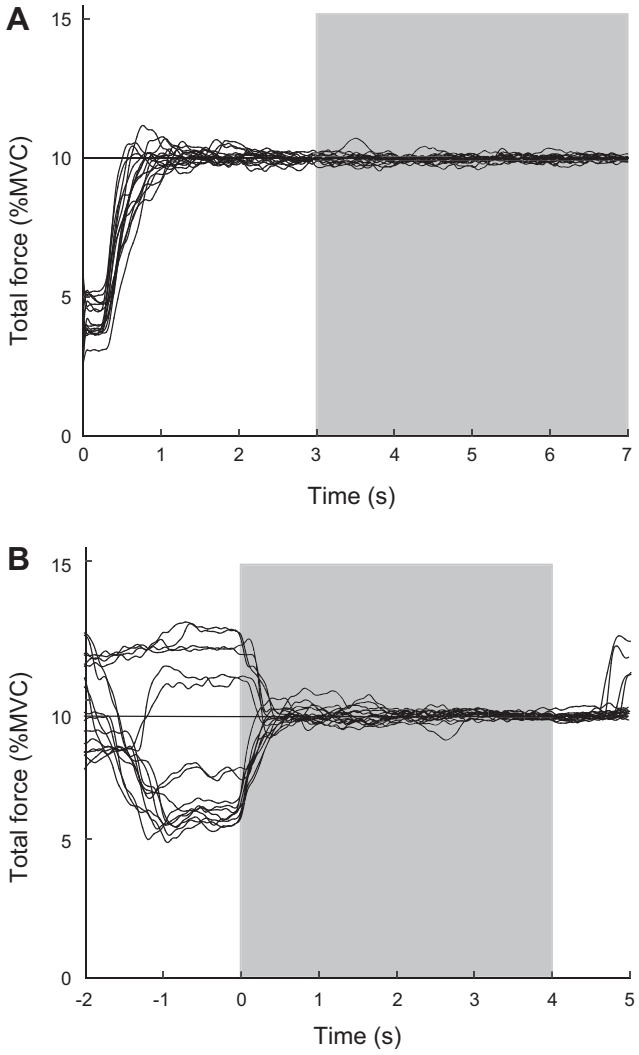

Fig. 3. Representative responses for the stable (*A*) and the slow dexterous (*B*) tasks. Each plot shows 16 separate trials. The last 4 s of the stable task (gray rectangle in *A*) were isolated and used for the UCM analysis. The trials for the slow dexterous trials were time-aligned so that the extended 10% MVC constant target-force portions began at the same instant. The first 4 s of the participant's responses (gray rectangle in *B*) were used for the UCM analysis.

UCM Analysis

Detailed description of the UCM analysis, in general (Latash et al. 2002; Scholz and Schöner 1999), and its application to multifinger force-production tasks, in particular, is found elsewhere (Latash et al. 2001; Scholz et al. 2003). The total force-production task is defined by the function $F_T = \Sigma F_i$; i = [index, middle, ring, little finger]. For each time instant, $t = t^*$, the individual finger forces across the 16 repetitions were isolated. The mean-subtracted individual finger forces (i.e., the input variables) were projected onto two orthogonal manifolds. The first manifold, called the uncontrolled manifold (UCM), is the null space of the Jacobian relating small changes in the input variables to small changes in the output (task) variable (F_T). Variance within the UCM has no influence on F_T. The second manifold, named ORT, is orthogonal to the UCM. Variance within this manifold influences F_T. The variances within these manifolds are called V_{UCM} and V_{ORT}, respectively. In the present experiment, the four input variables are constrained by a single task function. The Jacobian is obtained by computing the partial derivatives of the task function: J = [1 1 1 1]. The null space of this Jacobian, i.e., the UCM, is a three-dimensional linear space in the four-dimensional space of the input variables, and the ORT is a one-dimensional line orthogonal to the UCM. The dimension of ORT equals the number of constraints on the input variables, and the dimension of the UCM equals the number of input variables – number of constraints. The main output of the UCM analysis is the synergy index ΔV, which is defined as the relative amount of V_{UCM} in the total variance, V_{TOT}, normalized by the dimensions of the spaces in which the variances are computed: $\Delta V = [(V_{UCM}/3) - V_{ORT}]/(V_{TOT}/4)$.

The synergy index indicates whether the input variables (F_i) are coordinated to stabilize the task variable (F_T). A positive value of ΔV shows the presence of such coordination, a negative value of ΔV shows that the input variables are coordinated to change (i.e., destabilize) the task variable, and $\Delta V = 0$ implies that there is no task-specific coordination. Finally, a higher positive value of ΔV corresponds to stronger coordination and a greater stabilization of the task variable (F_T).

The synergy index is bounded: $-4 \leq \Delta V \leq 4/3$ ($\Delta V_{lower\text{-}bound} = -4$ when $V_{UCM} = 0$; $\Delta V_{upper\text{-}bound} = 4/3$ when $V_{ORT} = 0$). Therefore, for statistical analyses, the ΔV values were transformed using the Fisher z-transform adapted for the asymmetrical bounds (Zhou et al. 2013) to obtain the following:

$$\Delta Vz = 0.5\log\frac{4 + \Delta V}{1.33 - \Delta V}$$

Note that $\Delta V = 0$ implies $\Delta Vz = 0.5493$. Therefore, a ΔVz value greater than 0.5493 indicates the presence of a synergy that stabilizes F_T.

These computations were repeated for each time instant within the 4-s window, thus yielding the curves $V_{UCM}(t)$, $V_{ORT}(t)$, and $\Delta V(t)$ for each task type. An exponential function of the form $y(t) = ae^{(-t/\tau)} + b$ was fit in the least-squared sense to these curves for the slow and fast dexterous task types, where τ is the time constant in seconds, b is the steady-state value that the variable y reaches after infinite time, and a is the change in the value of y over that duration.

Statistics

Data are means ± SE, unless mentioned otherwise. The time constants τ obtained from the exponential fits to the $V_{ORT}(t)$ and $\Delta V(t)$ trajectories were subjected to paired-sample t-tests. The $V_{UCM}(t)$ trajectories did not resemble exponential functions (see RESULTS). The V_{UCM}, V_{ORT}, and z-transformed synergy index ΔVz values for two phases (*phase 1*, 2 to 3 s; *phase 2*, 3 to 4 s) were averaged within those time bins for each participant and subjected to separate two-way, repeated-measures ANOVAs with factors phase (2 levels) and task type (3 levels). To establish the presence of a synergy,

the ΔV_z values for the two phases and three task types were subjected to separate *t*-tests to test the null hypothesis: $\Delta V_z = 0.5493$. The V_{UCM} and V_{ORT} data were log-transformed to meet the normality requirement. However, nontransformed values are presented in the plots and as data in RESULTS. The phases were chosen on the basis of the time constants computed from the exponential fits to the temporal trajectories of these variables. The $V_{ORT}(t)$ curves attain over 99% of their steady-state value (*b*) by the end of 2 s for the slow and fast dexterous tasks. Similarly, the $\Delta V_z(t)$ curves reach 90% and 97% of their steady-state values by the 2- and 3-s mark, respectively, for the slow and fast dexterous tasks. Note that exponential fits to the $\Delta V_z(t)$ curves [rather than $\Delta V(t)$ curves] were utilized to compute the above estimates. Thus the dynamics associated with "settling" to the current task requirement (10% MVC) have been mostly damped by the end of 2 s, and therefore comparison with the stable task becomes reasonable. Mauchly's sphericity tests were performed to verify the validity of using repeated-measures ANOVA. The Greenhouse-Geisser adjustment to the degrees of freedom was applied whenever departure from sphericity was observed. Significant effects of ANOVA were further explored using pairwise comparisons with Bonferroni corrections. All possible pairwise contrasts were conducted. All statistics were performed using an α-level of 0.05 and with SPSS statistical software.

RESULTS

Performance of the Rapid Force Fluctuation Tasks

Recall that the participants produced rapid oscillations of the total force between 5% and 15% MVC targets. The across-participant mean (±SD) of the force peaks was 17.48 ± 3.09%MVC, that of the force valleys was 3.08 ± 1.44%MVC, and the mean force was 9.82 ± 1.93%MVC. The mean force rate production abilities of the participants were at least three times greater than those required by the slow and fast dexterous tasks. The across-participant maximum mean (±SD) of the absolute force rate was 379.59 ± 97.98%MVC/s, mean absolute force rate was 124.34 ± 37.42%MVC/s, and the oscillation frequency with maximum power was 4.26 ± 0.7 Hz. Most of the power in the target profiles (over 60%) was concentrated in the 0- to 2-Hz band, whereas the participants were capable of producing rapid force fluctuations at twice that frequency (~4 Hz). This indicates that the designed target-force profiles for the slow and fast dexterous tasks were well within the force-production abilities of the participants. Therefore, the participants' strength and finger force-production ability are unlikely to influence the results of this study.

Performance of the Stable and Slow and Fast Dexterous Tasks

Figure 3*A* depicts the performance of the stable task from a representative participant. The participants requires about 1 s to achieve the target (10% MVC), and then F_T remained stable about that target with some fluctuations. Figure 3*B* depicts the performance of the slow dexterous tasks from a representative participant. These data are aligned with respect to the start of the 10% MVC portions that last at least 4 s. Overall, the slow dexterous tasks elicited slower F_T responses than the fast dexterous tasks. The maximum absolute force rate was as follows: slow dexterous task (33.61 ± 7.6%MVC/s) < fast dexterous task (47.53 ± 8.53%MVC/s) [$t_{(24)} = -10.55$; $P < 0.01$]. The mean force rate was as follows: slow dexterous task (3.48 ± 0.5%MVC/s) < fast dexterous task (5.35 ± 0.91 %MVC/s) [$t_{(24)} = -15.477$; $P < 0.01$].

Despite the faster responses, the participants' performance was worse for the fast dexterous task. However, this is consistent with the designed differences between the slow and fast dexterous target profiles. Table 1 shows the output metrics of the cross-correlation between the target and response F_T curves averaged across the 16 repetitions and then the participants. The lag and the root-mean-squared error normalized by the mean force are larger, and the correlations are smaller for the fast dexterous task.

Time Evolution of the Variance Components and the Synergy Index

Figure 4 depicts the across-participant averaged behavior of the output variables from the UCM analysis for the stable, slow dexterous and the fast dexterous tasks. Recall these data are computed when the local task demands are identical (i.e., target $F_T = 10\%$ MVC). Data in Fig. 4, *A* and *C* [$\Delta V(t)$, $V_{UCM}(t)$, and $V_{ORT}(t)$ curves], are used for exponential function fitting, and the data in Fig. 4, *B* and *C* [$\Delta V_z(t)$, $V_{UCM}(t)$, and $V_{ORT}(t)$ curves] are used for the ANOVAs. The curves for the stable task show no variation with time, because the portion of the data chosen for this analysis was after the participants had reached the steady state (see Fig. 3*A*). In contrast, all variables for the slow and fast dexterous tasks show temporal variations: there is an exponential drop in V_{ORT} and an exponential increase in ΔV and ΔV_z. These initial changes reflect F_T convergence at different rates from different previous steady F_T targets to the 10% MVC target. The drop in V_{UCM} appears exponential, on average (Fig. 4*C*); however, the exponential fits to individual trajectories yielded low R^2 values (median $R^2 = 0.73$ and 0.79 for the slow and fast dexterous tasks, respectively). Initially, $\Delta V < 0$, indicating that the participants covary their finger forces positively to change F_T and achieve the required target of 10% MVC. The synergy index then changes sign, indicating that the finger forces switch from positive to negative covariation in a continuously increasing propensity to stabilize F_T. V_{ORT} drops rapidly during this period, and by the end of about 2 s, V_{ORT} for the slow and fast dexterous tasks is close to the value observed during the steady task (Fig. 4*D*). The key observation is that even after the convergence of V_{ORT}, both V_{UCM} and ΔV_z for the dexterous tasks are lower than the corresponding values for the stable task (Fig. 4, *C* and *B*, respectively).

All the above observations were supported by statistical analyses. The dynamics of F_T stabilization are captured and described by time constant τ of the exponential fits to the $\Delta V(t)$ and V_{ORT} (t) curves. For $\Delta V(t)$, the fits for the slow dexterous tasks yielded high R^2 values (median and interquartile range: 0.95 and 0.06, respectively), and $\tau = 0.30 \pm 0.02$ s (Fig. 4*A*).

Table 1. *Cross-correlation between target and response $F_T(t)$ traces for slow and fast dexterous tasks*

Metric	Slow Dexterous Performance	Fast Dexterous Performance	$t_{(24)}$	*P*
Lag, s	0.27 ± 0.03	0.32 ± 0.03	−9.832	<0.01
Correlation at zero lag	0.88 ± 0.01	0.54 ± 0.03	62.582	<0.01
Maximum correlation	0.96 ± 0.02	0.90 ± 0.02	13.665	<0.01
Normalized RMS error	0.11 ± 0.008	0.19 ± 0.008	−57.455	<0.01

Values are means ± SD across trials and participants.

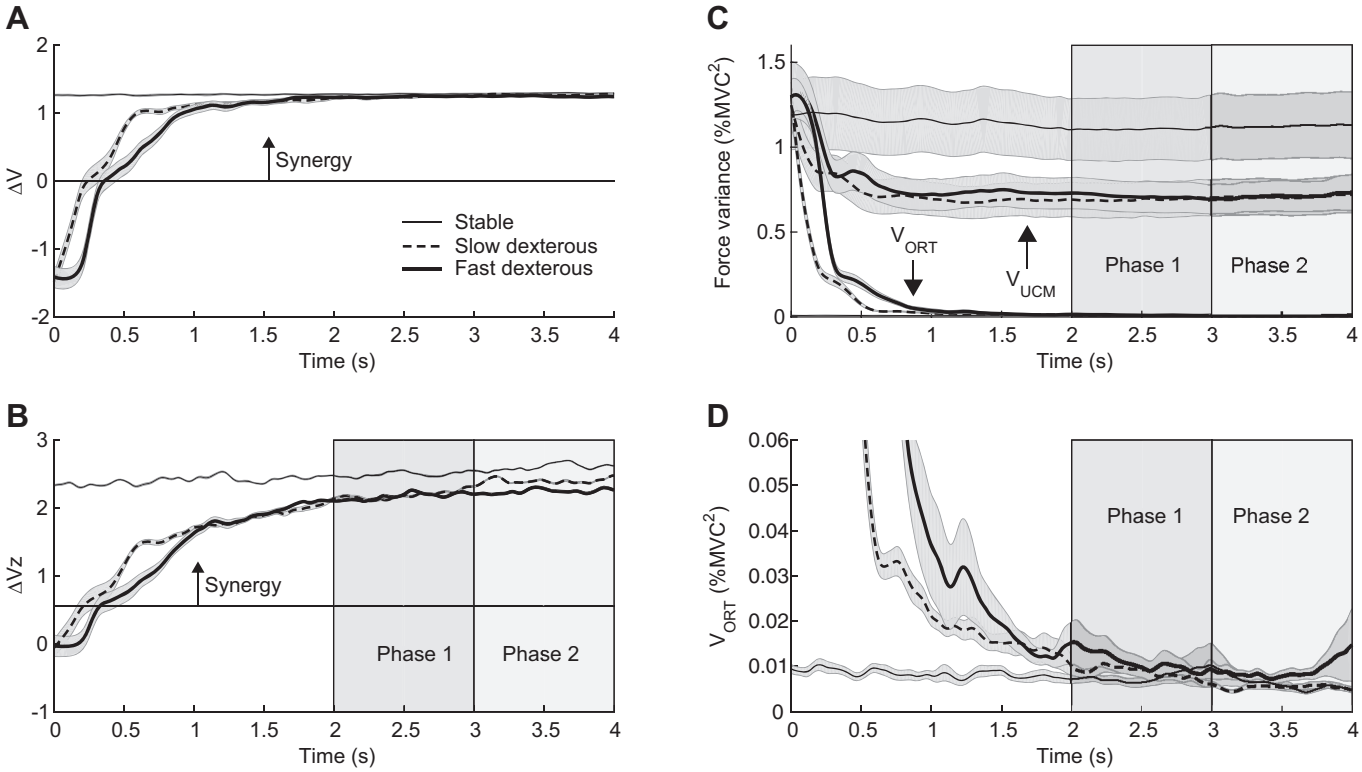

Fig. 4. Across-participant means ± SE of the synergy index (ΔV; *A*), *z*-transformed synergy index (ΔV*z*; *B*), and the variance components (V_{ORT} and V_{UCM}; *C*) are plotted against time. A close view of the orthogonal variance is shown in *D*. The variance components in *C* are not normalized by the number of dimensions of the corresponding spaces. ΔV > 0 (*A*) and ΔV*z* > 0.5493 (*C*) indicate the presence of synergy, stabilizing total force F_T.

The corresponding values for the fast dexterous task were $R^2 = 0.94$ and 0.03, respectively, and $\tau = 0.43 \pm 0.03$ s. The values for the V_{ORT} trajectories for the slow dexterous task were $R^2 = 0.97$ and 0.05, respectively, and $\tau = 0.16 \pm 0.01$ s. The values for the fast dexterous task were: $R^2 = 0.93$ and 0.03, respectively, and $\tau = 0.24 \pm 0.01$ s. Figure 4*D* shows the magnified view of these trajectories. Repeated-samples *t*-tests revealed significant differences for τ for ΔV [$\tau_{\Delta V\text{-slow-dexterous}} < \tau_{\Delta V\text{-fast-dexterous}}$; $t_{(24)} = -4.206$; $P < 0.01$], as well as V_{ORT} [$\tau_{Vort\text{-slow-dexterous}} < \tau_{Vort\text{-fast-dexterous}}$; $t_{(24)} = -3.902$; $P < 0.01$].

After the initial transients were exhausted, ΔV*z* for both dexterous tasks *1*) was greater than 0.5493, indicating the presence of a synergy stabilizing F_T, *2*) remained lower than that for the stable task, and *3*) continued to increase with time (Fig. 4*B*). Based on separate *t* tests on the averaged ΔV*z* values for each phase and task type, we rejected the null hypothesis that ΔV*z* = 0.5493 ($P < 0.01$). The mean ΔV*z* values were greater than 0.5493. The two-way, phase × task type ANOVA revealed a significant effect of task type [$F_{(2,48)} = 13.794$; $P < 0.01$; partial $\eta^2 = 0.365$]. Pairwise comparisons revealed ΔVz_{stable} (2.55 ± 0.07) > $\Delta Vz_{slow\text{-}dexterous}$ (2.29 ± 0.08) and ΔVz_{stable} > $\Delta Vz_{fast\text{-}dexterous}$ (2.21 ± 0.07). There was also a significant effect of phase [$F_{(1,24)} = 21.953$; $P < 0.01$; partial $\eta^2 = 0.478$]. Pairwise comparisons revealed $\Delta Vz_{Phase\text{-}1}$ (2.29 ± 0.06) < $\Delta Vz_{Phase\text{-}2}$ (2.41 ± 0.06). The interaction was close to significant [$F_{(2,48)} = 2.981$; $P = 0.06$; partial $\eta^2 = 0.11$], and it suggested that the increase in ΔV*z* across the phases tends to be slower for fast dexterous task compared with the other two tasks (Fig. 5*A*).

The V_{UCM} values were significantly lower for the dexterous tasks compared with the stable tasks, but they did not show any change with phase. The two-way ANOVA revealed a significant effect of task type [$F_{(2,48)} = 6.225$; $P < 0.01$; partial $\eta^2 = 0.206$] but no effect of phase ($P = 0.385$) or any interaction ($P = 0.723$) (Fig. 5*B*). Pairwise comparisons revealed $V_{UCM\text{-}stable}$ (1.11 ± 0.18%MVC^2) > $V_{UCM\text{-}slow\text{-}dexterous}$ (0.70 ± 0.1%MVC^2) and $V_{UCM\text{-}stable}$ > $V_{UCM\text{-}fast\text{-}dexterous}$ (0.71 ± 0.09%MVC^2); this comparison was close to significance ($P = 0.06$).

The V_{ORT} values continued to decrease across phase, but there was no significant difference across task type ($P = 0.074$). The two-way ANOVA revealed a main effect of phase for V_{ORT} [$F_{(1,24)} = 20.586$; $P < 0.01$; partial $\eta^2 = 0.462$]. Pairwise comparisons revealed $V_{ORT\text{-}Phase\text{-}1}$ (0.009 ± 0.001 %MVC^2) > $V_{ORT\text{-}Phase\text{-}2}$ (0.007 ± 0.001%MVC^2). There was also a significant task type × phase interaction [$F_{(2,48)} = 3.416$; $P = 0.041$; partial $\eta^2 = 0.125$], which reflects the greater across-phase decrease in V_{ORT} for the fast dexterous tasks compared with that for the slow dexterous task (Fig. 5*C*).

DISCUSSION

The data support one of the two hypotheses formulated in the Introduction. *Hypothesis 1* aimed to establish the effect of cuing on stability. It stated that the synergy index (ΔV: our measure for stability) would be lower for the slow and fast dexterous tasks when the participant expected to change F_T, compared with the stable task when they did not expect to change F_T, despite the uncertain timing of the upcoming state change in the dexterous tasks. Indeed, the steady-state ΔV*z*

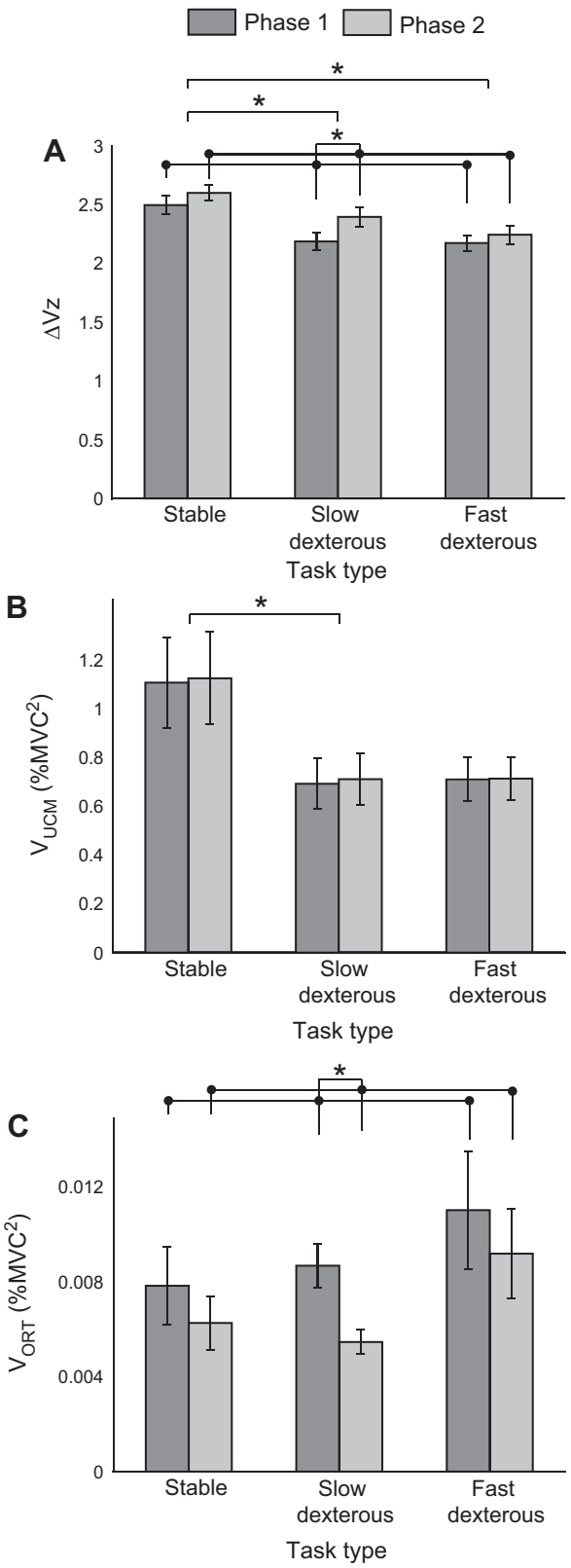

Fig. 5. Values are means ± SE of the z-transformed synergy index ΔV_z (*A*), V_{UCM} (*B*), and V_{ORT} (*C*) across task types and phases. V_{UCM} is not normalized by the dimension of the UCM space.

values for the dexterous tasks were lower by ~12% than those for the stable task after the dynamics associated with converging to the 10% MVC target were dissipated (Fig. 5*A*).

Hypothesis 2 predicted that the change in stability would scale with the difficulty of the task, and therefore, the drop in ΔV would be greater for the fast dexterous task. We did not find compelling evidence to support this hypothesis. On the one hand, the time constant τ for $\Delta V(t)$ for the slow dexterous task (~0.3 s) was shorter than that for the fast dexterous task (~0.43 s). This suggests that convergence to the steady-state ΔV value was faster for the slow dexterous task, despite the fact that the $F_T(t)$ response during the slow dexterous task was slower, on average (the mean force rate for the slow dexterous task is significantly lower). On the other hand, there was no significant difference in the ΔV_z values for the slow and the fast dexterous tasks in *phases 1* and *2* (Figs. 4*B* and 5*A*), and the phase × task type interaction for ΔV_z was not significant ($P = 0.06$).

The two variance components, V_{UCM} and V_{ORT}, influence ΔV. To investigate the causes for the changes in ΔV, we explored the changes in these variance components and obtained two striking observations. First, a drop in V_{UCM} (~37%; Fig. 4*C*) was responsible for the drop in ΔV for the dexterous tasks, and second, after the convergence to the 10% MVC target was achieved, there was no significant difference in V_{ORT} across the task types (Fig. 4*D*). Below, we discuss the implications of these findings and other relevant issues.

The Two Stages of Anticipatory Synergy Adjustments

Note that during the 4-s window of the dexterous tasks for which ΔV was computed, the anticipated divergence from the 10% MVC target never occurred. The target remained stationary, meaning that the participants never transitioned from the state of preparedness to transitioning between states. This is in stark contrast with all previous ASA studies in which ΔV was computed immediately preceding a state change. Therefore, the main result of the present study demonstrates that ASA is a two-stage process, as depicted in Fig. 6. ΔV drops during both stages, triggered by different environmental events and via different mechanisms. When the participant expects no change in the steady-state behavior, the stability of the current state is high. This is depicted as the shaded ellipse, and it is reflected in the relations $V_{UCM} > V_{ORT}$ and $\Delta V > 0$. The present study documents, for the first time, the first process, stage 1 ASA, which occurs during the foreperiod in response to a cue that primes the participant for a possible rapid movement in the near future. Here, V_{UCM} decreases significantly and V_{ORT} remains invariant (ellipse with the bold solid edge in Fig. 6), which leads to a decrease in ΔV. However, $\Delta V > 0$, indicating that the current state has lower stability, but it is not unstable. Stage 1 ASA occurs regardless of the nature of the uncertainty in the upcoming task. In contrast, previous studies have discovered and documented stage 2 ASA, which begins ~150–400 ms before the instant when the task variable changes. They occur only in response to a temporal cue to produce changes in task variables that is provided sufficiently in advance, but not otherwise (Olafsdottir et al. 2005; Shim et al. 2006; Zhou et al. 2013). During stage 2 ASA, V_{ORT} increases, V_{UCM} may show a small decrease or increase (Arpinar-Avsar et al. 2013; Jo et al. 2017; Klous et al. 2011), and ΔV decreases further (ellipse

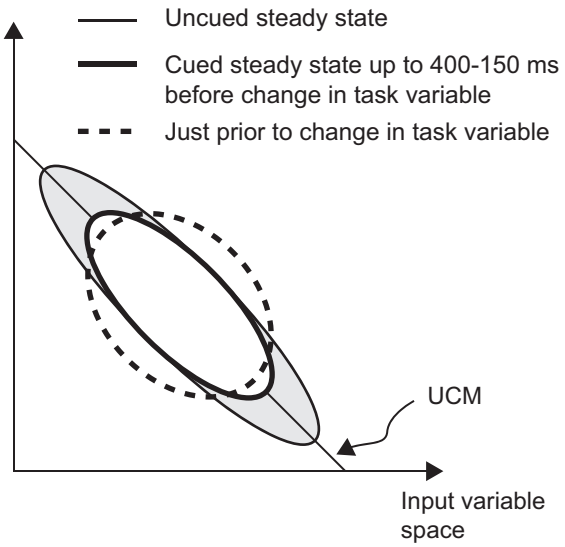

Fig. 6. Two stages of anticipatory synergy adjustments. The reference frame represents *n*-dimensional space of the input variables, the inclined line represents the UCM, and the ellipses depict variability distributions during various phases leading up to a change in the output task variable.

with the dashed edge in Fig. 6). ΔV eventually becomes negative, the system transitions from being stable to unstable, and the output variable begins to change.

Conceived this way, the duration of ASAs is much longer than that reported previously by Latash and colleagues (cf. Latash and Huang 2015). As seen in Fig. 4*D*, after ~2.5 s, V_{ORT} for the dexterous tasks resembles that for the stable task, and ΔV values for the dexterous tasks have stabilized (Fig. 4*A*). The ΔV values remain lower than that for the stable task for the remaining 1.25 s, and this difference will likely persist for some more time if the target F_T trajectory remains invariant. Even with this conservative estimate, stage 1 ASA recorded here are about five times longer than the stage 2 ASAs summarized by Latash and Huang (2015) (150–250 ms) and over three times longer than the 400-ms stage 2 ASA reported by Togo and Imamizu (2016).

Finally, this study provides evidence, although not as strong, suggesting that stage 1 ASA scales in response to the perceived difficulty of the task. This scaling is reflected in the longer time constant of the ΔV(*t*) curve for the fast dexterous task compared with the slow dexterous task. Note that scalability of stage 2 ASA has not been addressed before. The extent and the resolution with which stability can be modulated remain to be established.

Changes in Variance Components

Changes in V_{UCM}. Why does V_{UCM} drop during stage 1 ASA? We provide two possible explanations. First, the reduction in V_{UCM} implies more stereotypical sharing of the total force among the input finger forces. Whereas cuing reduced V_{UCM} in the present study despite the uncertainty, previous studies have demonstrated that in the cued condition, introducing uncertainty into the upcoming motor actions leads to an increase in V_{UCM} (de Freitas et al. 2007; Freitas and Scholz 2009). Together, these studies suggest the following relations: V_{UCM} when a well-defined motion is expected $< V_{UCM}$ when motion of an unknown nature is expected $< V_{UCM}$ when no motion is expected. A coherent, but speculative, account of these relations is obtained by extending the argument of de Freitas et al. (2007), who note that it is unlikely that the entire UCM is utilized during any behavior. Rather, a subset of configurations within the UCM facilitate transitions to other configurations by making them efficient in some sense (e.g., faster response time). When a state change is expected and the target is known a priori, the CNS restricts the system's current state to this subset. Furthermore, the "efficient" subsets may be different for different targets to which the system may transition. Therefore, when the target is uncertain, the CNS may allow the system to occupy configurations that belong to the union of the subsets associated with all possible targets, leading to the increased V_{UCM} in the cued but uncertain target condition. We further speculate that when the CNS expects no movement, it imposes fewer restrictions on the states that the system can occupy within the UCM, which leads to even greater amount of V_{UCM}.

Second, in controlled isometric conditions, such as those in this experiment, the variability in the inputs arises primarily from neuromuscular noise, and a positive ΔV indicates that a larger portion of the noise is channeled into the UCM. Presumably, for similar system configuration and CNS control, volitional action and responses to external disturbances will also display this characteristic variability structure (Martin et al. 2009; Scholz and Schöner 2014). Studies on reaching movement (Mattos et al. 2011, 2013; Scholz et al. 2011), finger force production (Ambike et al. 2016; Mattos et al. 2015; Wilhelm et al. 2013), and postural control (Scholz et al. 2007) provide evidence that both voluntary and perturbation-induced movements indeed have significant components along the UCM. Note that during voluntary movement, the UCM component, known as self-motion (Burdick 1989; Nenchev 1992; Scholz and Schöner 2014), is detrimental to the system's agility because it is simply fails to produce the desired movement in the task variables. Therefore, in the present study, the drop in V_{UCM}, combined with the invariant V_{ORT}, ensures that a larger component of any volitional neural command will effect a change in the system's current state.

In conclusion, smaller V_{UCM} for the dexterous tasks implies *1*) tighter control over the current system state and *2*) a reduction in the amount of self-motion. In this way, smaller V_{UCM} facilitates rapid task switching, i.e., dexterity.

Changes in V_{ORT}. A small increase in V_{ORT} is apparent for the dexterous tasks compared with the stable task in Fig. 4*D*. These trends failed to reach statistical significance. Nevertheless, they appear to predict the changes in V_{ORT} that follow when the state transition takes place. Increased V_{ORT} is observed in self-paced actions in isometric finger force-production tasks (Shim et al. 2005; Togo and Imamizu 2016) as well as postural tasks (Piscitelli et al. 2017). Furthermore, an increase in V_{ORT} is more commonly the cause for the drop in synergy index ΔV associated with stage 2 ASA (Arpinar-Avsar et al. 2013; Jo et al. 2017; Klous et al. 2011). Therefore, it is likely that the small changes in V_{ORT} in stage 1 ASA will eventually become large during stage 2 ASA.

Changes in the total variance. Note that the total variance in the input variables is $V_{TOT} = V_{UCM} + V_{ORT}$. Therefore, the large decrease in V_{UCM} and minimal change in V_{ORT} imply that the total variance in the finger forces has decreased, and it is associated with lower stability (lower ΔV) for the dexterous tasks. This may seem contradictory, because lower variability

is often considered a consequence of higher stability. However, the relation between variability and stability is subtle (van Emmerik and van Wegen 2000). For example, fall history in older adults is associated with both too much and too little step width variability (Brach et al. 2005); persons with Parkinson's disease simultaneously display lower variability in their upright postural sway and lower postural stability (Horak et al. 1992). For the dexterous tasks in the present study, we have argued that the system is functioning in configurations that facilitate departures from the current state. Therefore, it is conceivable that tight control over these states is maintained to minimize the chances of false starts.

To illustrate the changes in the variance components, imagine a 100-m runner at the start line of a race. The runner is cued for a transition from a (barely) stable static posture into a dynamically stable gait. However, the moment of the transition is unknown. The runner assumes a rather specific posture that places her center of mass close to the boundary of the base of support to facilitate a rapid transition into running. She has not only lowered the stability of her current state, she has also constrained her whole body kinematic configuration to a small subset of the set of all possible stable configurations with the feet and hands in contact with the ground. In other words, her posture is minimally stable and has small V_{UCM} at the same time. Furthermore, she exerts tight control over V_{ORT} and V_{TOT} to maintain her precarious posture and to ensure minimal self-motion during the transition to the gait.

Possible Mechanisms for Stability Modulation in Redundant Systems

Neurophysiological mechanisms for synergies and ASA remain unidentified. Various researchers have proposed feedforward and feedback models that can generate task-specific structured variability in the input variables, and there exist mechanisms that plausibly instantiate in the human body the principles that the models describe. The theoretical models include optimal feedback control schemes (Todorov and Jordan 2002), schemes using central back-coupling loops (Latash et al. 2005), and a scheme that unites the control of salient task variables with referent coordinates (Feldman 2011) and feedback loops (Martin et al. 2009). Examples of neurophysiological mechanisms include the well-known system of Renshaw cells, which could be the central back-coupling loop that generates a synergy stabilizing the output of the corresponding motoneuronal pool without the use of afferent feedback. In contrast, the tonic stretch reflex may be seen as a synergy that relies on peripheral feedback and stabilizes the equilibrium between the muscle and external load (Latash 2008).

Moving from synergy to ASA, Goodman and Latash (2006) constructed a model that uses only feedforward control and achieves stage 2 ASA. In particular, by allowing greater variance in the assumed input variables, the model generates similar overall performance of the task (no change in the output variable) but reduces ΔV. This view is consistent with the dynamic systems approach to task switching, which assumes that that motor behavior emerges from the combined deterministic and random processes (Riley and Turvey 2002). Changes in movement patterns arise as an influx of random noise into the system destabilizes the current pattern and facilitates a transition to a new one (Kiefer and Myer 2015). It is possible that a mixture of feedback and feedforward mechanisms are employed for establishing synergies and modulating their strength for varying task requirements.

It is likely that cortical, subcortical, and spinal structures generate cue-induced stage 1 ASA. Cortical involvement is suggested by the slow negative wave in the electroencephalogram (Brunia et al. 2012), known as the readiness potential (RP) that accompanies an expectation of movement. Herrmann et al. (2008) have shown that the RP appears in response to the mere expectation of movement even when the participant is unable to decide which movement to perform. Furthermore, Churchland et al. (2006) recorded neural firing rates from the dorsal premotor cortex in monkeys and demonstrated a significant decrease in across-trial variability during the foreperiod of a delay-reach task. This finding is similar to the decline in V_{UCM} (and V_{TOT}) during the foreperiod of the dexterous tasks seen in our study. Churchland et al. (2006) interpreted this result as motor preparation and proposed the optimal subspace hypothesis, much in the same vein as one explanation provided in the present study for the decrease in V_{UCM}. This hypothesis states that there exists in the space of firing rates of all neurons, a subspace of states that is optimal for producing specific desired movements. Motor preparation consists in constraining the neural firing rates to lie within the optimal subspace for the desired movement. This leads to the observed decline in variability. Next, the cortex is thought to receive subcortical motor information gated through the thalamus, especially during the foreperiod (Brunia 1993). Finally, supraspinal control of the gain of spinal reflexes could also contribute to the appearance of cue-induced stage 1 ASA. This is consistent with the well-known increase in muscle tone in anticipation of movement (Sherrington 1906) and changes in spinal reflexes during the foreperiod in cued simple reaction-time tasks. Although these changes vary depending on task complexity, there is evidence of increased reflexes in the agonist muscles (reviewed in Prochazka 1989). In particular, consistent with the prolonged decrease in ΔV during the foreperiod, sustained augmentation in the Hoffman and tendon-jerk reflexes has been observed for up to 4 s before movement during the foreperiod (Scheirs and Brunia 1985).

RP and modulations in the gains of spinal reflexes are observed in choice reaction-time tasks for movements with a single actuator, or homologous, bilateral actuators (e.g., button presses with the left or right finger). To the best of our knowledge, these phenomena have not been investigated in the context of actions performed using redundant sets of actuators. It is tempting to hypothesize that cue-induced stage 1 ASA is the physical, downstream manifestation of the RP and/or the reduced variability in the neuronal firing rates in the premotor cortical areas, mediated in part by alterations in the gains of spinal reflexes.

Stability Modulation Mediates the Stability-Dexterity Conflict

A key aspect of dexterity is the ability to transition between behaviors in response to changing task demands (Bernstein 1996). This sets up a conflict between dexterity and stability, the ability of the motor system to maintain the current static or dynamic state. Although several researchers have highlighted the dexterity-stability clash (Hasan 2005; Latash and Huang 2015; Riccio 1993; Riccio and Stoffregen 1988; Riley and

Turvey 2002), investigations to understand how the CNS resolves the conflict continue.

Although it has been argued that ASA facilitates dexterous behavior (Robert et al. 2009; Shim et al. 2005), direct evidence that relates reduction in ΔV with gains in subsequent task performance are lacking. One key exception is the study by Togo and Imamizu (2016), who imposed accuracy requirements on the generated force pulse magnitude in an isometric finger force-production task and demonstrated that ASA begins earlier (400 ms) and that earlier ASA is associated with greater precision in the generated force pulse. In the present study, the evidence does not suggest that the reduced stability for the fast dexterous task improved dexterous task switching. Rather, the tracking performance, global and local (immediately following the extend portion of 10% MVC), was worse for the fast dexterous task compared with the slow dexterous task. This is the main drawback of this work. It is likely that the increased difficulty of the fast dexterous task washed out the benefit, and the performance of that task would be even worse had the stability not been modulated. However, these are speculations that need further investigation. Another limitation is that our manipulation of speed (slow vs. fast dexterous tasks) was perhaps not effective at generating a difference in the perceived difficulty of the task. There was no significant difference in ΔV for these two task types, nor was there a significant phase $\times$ task type interaction. Therefore, although we suspect that stability modulation is a graded phenomenon, we are unable to demonstrate this at present.

It must be noted that additional factors likely influence the resolution of the stability-dexterity conflict. In bipedal locomotion studies, the kinematic synergy of the lower limb joints stabilizing the position of the foot weakens before heel strike (Robert et al. 2009; Rosenblatt et al. 2014, 2015). The weaker synergy presumably ensures adaptability in foot placement, although the need for such adaptability is unclear. Wu et al. (2015) identified general anticipatory preparations for changing the direction of forward locomotion to the left or to the right in response to an external visual cue. When the timing of the upcoming change was known but its direction was unknown, participants increased the lateral margin of stability two steps before the presentation of the cue. The stability was computed as the distance between the center-of-mass location and the lateral boundary of the base of support, and this method does not account for the redundant structure of the lower limbs. Nevertheless, this result is counter to the evidence presented in this report, and it suggests that the resolution of the stability-dexterity conflict may be influenced by safety considerations.

Finally, despite their ignorance, it is plausible that the participants guessed the presence of the 10% MVC steady state in the dexterous tasks after a few repetitions. To check for this possibility, we computed V_{UCM}, V_{ORT}, and ΔVz using the first eight trials and then again using the last eight trials for each subject and for slow and fast dexterous tasks. The three variables were subjected to separate three-way repeated-measures task type $\times$ phase $\times$ adaptation ANOVAs. Adaptation had two levels, early (first 8 trials) and late (last 8 trials). None of the variables showed a main effect of adaptation (V_{UCM}: $P = 0.157$; V_{ORT}: $P = 0.482$; ΔVz: $P = 0.157$) or any interactions. We conclude that there was no adaptation across trial number.

In conclusion, we have demonstrated that *1*) cuing a participant for an upcoming manual, isometric force-production task reduces the stability of the current motor state (12%), *2*) the reduction in stability occurs despite the uncertainty in the nature and the timing of the upcoming task, and *3*) the reduction in stability is associated with a substantial reduction (37%) in the variance along the uncontrolled manifold (V_{UCM}). We have argued that the reduction in stability and V_{UCM} can enhance dexterous responses to changing task demands. We have also argued that this stability reduction is stage 1 anticipatory synergy adjustment, and it is independent of the stage 2 version of the same phenomenon reported over the past decade (reviewed in Latash and Huang 2015).

DISCLOSURES

No conflicts of interest, financial or otherwise, are declared by the authors.

AUTHOR CONTRIBUTIONS

S.S.A. conceived and designed research; M.T. performed experiments; S.S.A. and M.T. analyzed data; S.S.A. and M.T. interpreted results of experiments; S.S.A. prepared figures; S.S.A. and M.T. drafted manuscript; S.S.A. and M.T. edited and revised manuscript; S.S.A. and M.T. approved final version of manuscript.

REFERENCES

Ambike S, Mattos D, Zatsiorsky VM, Latash ML. Synergies in the space of control variables within the equilibrium-point hypothesis. *Neuroscience* 315: 150–161, 2016. doi:10.1016/j.neuroscience.2015.12.012.

Arpinar-Avsar P, Park J, Zatsiorsky VM, Latash ML. Effects of muscle vibration on multi-finger interaction and coordination. *Exp Brain Res* 229: 103–111, 2013. doi:10.1007/s00221-013-3597-y.

Bernstein NA. *The Coordination and Regulation of Movements*. Oxford: Pergamon, 1967.

Bernstein NA. *On Dexterity and Its Development*. Mahwah, NJ: Lawrence Erlbaum, 1996.

Brach JS, Berlin JE, VanSwearingen JM, Newman AB, Studenski SA. Too much or too little step width variability is associated with a fall history in older persons who walk at or near normal gait speed. *J Neuroeng Rehabil* 2: 21, 2005. doi:10.1186/1743-0003-2-21.

Brunia CH. Waiting in readiness: gating in attention and motor preparation. *Psychophysiology* 30: 327–339, 1993. doi:10.1111/j.1469-8986.1993.tb02054.x.

Brunia CH, Geert JM, Bocker KE. Negative slow waves as indices of anticipation: the Bereitschaftspotential, the contingent negative variation, and the stimulus-preceding negativity. In: *The Oxford Handbook of Event-Related Potential Components*, edited by Kappenman ES and Luck SJ. Oxford: Oxford University Press, 2012, p. 189–207.

Burdick JW. On the inverse kinematics of redundant manipulators: characterization of the self-motion manifolds. In: *Proceedings, International Conference on Robotics and Automation* 1989, vol. 261, p. 264–270.

Churchland MM, Yu BM, Ryu SI, Santhanam G, Shenoy KV. Neural variability in premotor cortex provides a signature of motor preparation. *J Neurosci* 26: 3697–3712, 2006. doi:10.1523/JNEUROSCI.3762-05.2006.

de Freitas SM, Scholz JP, Stehman AJ. Effect of motor planning on use of motor abundance. *Neurosci Lett* 417: 66–71, 2007. doi:10.1016/j.neulet.2007.02.037.

Dingwell JB, John J, Cusumano JP. Do humans optimally exploit redundancy to control step variability in walking? *PLOS Comput Biol* 6: e1000856, 2010. doi:10.1371/journal.pcbi.1000856.

Feldman AG. Space and time in the context of equilibrium-point theory. *Wiley Interdiscip Rev Cogn Sci* 2: 287–304, 2011. doi:10.1002/wcs.108.

Freitas SMSF, Scholz JP. Does hand dominance affect the use of motor abundance when reaching to uncertain targets? *Hum Mov Sci* 28: 169–190, 2009. doi:10.1016/j.humov.2009.01.003.

Goodman D, Kelso JA. Are movements prepared in parts? Not under compatible (naturalized) conditions. *J Exp Psychol Gen* 109: 475–495, 1980. doi:10.1037/0096-3445.109.4.475.

Goodman SR, Latash ML. Feed-forward control of a redundant motor system. *Biol Cybern* 95: 271–280, 2006. doi:10.1007/s00422-006-0086-4.

Hasan Z. The human motor control system's response to mechanical perturbation: should it, can it, and does it ensure stability? *J Mot Behav* 37: 484–493, 2005. doi:10.3200/JMBR.37.6.484-493.

Herrmann CS, Pauen M, Min BK, Busch NA, Rieger JW. Analysis of a choice-reaction task yields a new interpretation of Libet's experiments. *Int J Psychophysiol* 67: 151–157, 2008.

Horak FB, Nutt JG, Nashner LM. Postural inflexibility in parkinsonian subjects. *J Neurol Sci* 111: 46–58, 1992. doi:10.1016/0022-510X(92)90111-W.

Jahanshahi M, Brown RG, Marsden CD. Simple and choice reaction time and the use of advance information for motor preparation in Parkinson's disease. *Brain* 115: 539–564, 1992. doi:10.1093/brain/115.2.539.

Jo HJ, Mattos D, Lucassen EB, Huang X, Latash ML. Changes in multidigit synergies and their feed-forward adjustments in multiple sclerosis. *J Mot Behav* 49: 218–228, 2017. doi:10.1080/00222895.2016.1169986.

Kiefer AW, Myer GD. Training the antifragile athlete: a preliminary analysis of neuromuscular training effects on muscle activation dynamics. *Nonlinear Dynamics Psychol Life Sci* 19: 489–510, 2015.

Kim SW, Shim JK, Zatsiorsky VM, Latash ML. Anticipatory adjustments of multi-finger synergies in preparation for self-triggered perturbations. *Exp Brain Res* 174: 604–612, 2006. doi:10.1007/s00221-006-0505-8.

Klous M, Mikulic P, Latash ML. Two aspects of feedforward postural control: anticipatory postural adjustments and anticipatory synergy adjustments. *J Neurophysiol* 105: 2275–2288, 2011. doi:10.1152/jn.00665.2010.

Körding KP, Wolpert DM. Bayesian integration in sensorimotor learning. *Nature* 427: 244–247, 2004. doi:10.1038/nature02169.

Krishnan V, Aruin AS, Latash ML. Two stages and three components of the postural preparation to action. *Exp Brain Res* 212: 47–63, 2011. doi:10.1007/s00221-011-2694-z.

Latash ML. *Synergy*. New York: Oxford University Press, 2008. doi:10.1093/acprof:oso/9780195333169.001.0001.

Latash ML. The bliss (not the problem) of motor abundance (not redundancy). *Exp Brain Res* 217: 1–5, 2012. doi:10.1007/s00221-012-3000-4.

Latash ML, Huang X. Neural control of movement stability: lessons from studies of neurological patients. *Neuroscience* 301: 39–48, 2015. doi:10.1016/j.neuroscience.2015.05.075.

Latash ML, Scholz JF, Danion F, Schöner G. Structure of motor variability in marginally redundant multifinger force production tasks. *Exp Brain Res* 141: 153–165, 2001. doi:10.1007/s002210100861.

Latash ML, Scholz JP, Schöner G. Motor control strategies revealed in the structure of motor variability. *Exerc Sport Sci Rev* 30: 26–31, 2002. doi:10.1097/00003677-200201000-00006.

Latash ML, Scholz JP, Schöner G. Toward a new theory of motor synergies. *Mot Contr* 11: 276–308, 2007. doi:10.1123/mcj.11.3.276.

Latash ML, Shim JK, Smilga AV, Zatsiorsky VM. A central back-coupling hypothesis on the organization of motor synergies: a physical metaphor and a neural model. *Biol Cybern* 92: 186–191, 2005. doi:10.1007/s00422-005-0548-0.

Martin V, Scholz JP, Schöner G. Redundancy, self-motion, and motor control. *Neural Comput* 21: 1371–1414, 2009. doi:10.1162/neco.2008.01-08-698.

Mattos D, Kuhl J, Scholz JP, Latash ML. Motor equivalence (ME) during reaching: is ME observable at the muscle level? *Mot Contr* 17: 145–175, 2013. doi:10.1123/mcj.17.2.145.

Mattos D, Schöner G, Zatsiorsky VM, Latash ML. Task-specific stability of abundant systems: Structure of variance and motor equivalence. *Neuroscience* 310: 600–615, 2015. doi:10.1016/j.neuroscience.2015.09.071.

Mattos DJ, Latash ML, Park E, Kuhl J, Scholz JP. Unpredictable elbow joint perturbation during reaching results in multijoint motor equivalence. *J Neurophysiol* 106: 1424–1436, 2011. doi:10.1152/jn.00163.2011.

Müller H, Sternad D. Motor learning: changes in the structure of variability in a redundant task. In: *Progress in Motor Control*, edited by Sternad D. Boston, MA: Springer, 2009, p. 439–456. doi:10.1007/978-0-387-77064-2_23.

Nenchev DN. Restricted Jacobian matrices of redundant manipulators in constrained motion tasks. *Int J Rob Res* 11: 584–597, 1992. doi:10.1177/027836499201100608.

Niemi P, Naatanen R. Foreperiod and simple reaction-time. *Psychol Bull* 89: 133–162, 1981. doi:10.1037/0033-2909.89.1.133.

Olafsdottir H, Yoshida N, Zatsiorsky VM, Latash ML. Anticipatory covariation of finger forces during self-paced and reaction time force production. *Neurosci Lett* 381: 92–96, 2005. doi:10.1016/j.neulet.2005.02.003.

Olafsdottir H, Yoshida N, Zatsiorsky VM, Latash ML. Elderly show decreased adjustments of motor synergies in preparation to action. *Clin Biomech (Bristol, Avon)* 22: 44–51, 2007. doi:10.1016/j.clinbiomech.2006.08.005.

Olafsdottir HB, Kim SW, Zatsiorsky VM, Latash ML. Anticipatory synergy adjustments in preparation to self-triggered perturbations in elderly individuals. *J Appl Biomech* 24: 175–179, 2008. doi:10.1123/jab.24.2.175.

Park J, Wu YH, Lewis MM, Huang X, Latash ML. Changes in multifinger interaction and coordination in Parkinson's disease. *J Neurophysiol* 108: 915–924, 2012. doi:10.1152/jn.00043.2012.

Piscitelli D, Falaki A, Solnik S, Latash ML. Anticipatory postural adjustments and anticipatory synergy adjustments: preparing to a postural perturbation with predictable and unpredictable direction. *Exp Brain Res* 235: 713–730, 2017. doi:10.1007/s00221-016-4835-x.

Prochazka A. Sensorimotor gain control: a basic strategy of motor systems? *Prog Neurobiol* 33: 281–307, 1989. doi:10.1016/0301-0082(89)90004-X.

Riccio GE. Information in movement variability about quantitative dynamics of posture and orientation. In: *Variability and Motor Control*, edited by Newell KM and Corcos DM. Champaign, IL: Human Kinetics, 1993, p. 317–357.

Riccio GE, Stoffregen TA. Affordances as constraints on the control of stance. *Hum Mov Sci* 7: 265–300, 1988. doi:10.1016/0167-9457(88)90014-0.

Riley MA, Turvey MT. Variability and determinism in motor behavior. *J Mot Behav* 34: 99–125, 2002. doi:10.1080/00222890209601934.

Robert T, Bennett BC, Russell SD, Zirker CA, Abel MF. Angular momentum synergies during walking. *Exp Brain Res* 197: 185–197, 2009. doi:10.1007/s00221-009-1904-4.

Rosenblatt NJ, Hurt CP, Latash ML, Grabiner MD. An apparent contradiction: increasing variability to achieve greater precision? *Exp Brain Res* 232: 403–413, 2014. doi:10.1007/s00221-013-3748-1.

Rosenblatt NJ, Latash ML, Hurt CP, Grabiner MD. Challenging gait leads to stronger lower-limb kinematic synergies: the effects of walking within a more narrow pathway. *Neurosci Lett* 600: 110–114, 2015. doi:10.1016/j.neulet.2015.05.039.

Santisteban L, Térémetz M, Bleton JP, Baron JC, Maier MA, Lindberg PG. Upper limb outcome measures used in stroke rehabilitation studies: a systematic literature review. *PLoS One* 11: e0154792, 2016. doi:10.1371/journal.pone.0154792.

Scheirs JG, Brunia CH. Achilles tendon reflexes and surface EMG activity during anticipation of a significant event and preparation for a voluntary movement. *J Mot Behav* 17: 96–109, 1985. doi:10.1080/00222895.1985.10735339.

Scholz JP, Dwight-Higgin T, Lynch JE, Tseng YW, Martin V, Schöner G. Motor equivalence and self-motion induced by different movement speeds. *Exp Brain Res* 209: 319–332, 2011. doi:10.1007/s00221-011-2541-2.

Scholz JP, Kang N, Patterson D, Latash ML. Uncontrolled manifold analysis of single trials during multi-finger force production by persons with and without Down syndrome. *Exp Brain Res* 153: 45–58, 2003. doi:10.1007/s00221-003-1580-8.

Scholz JP, Schöner G. The uncontrolled manifold concept: identifying control variables for a functional task. *Exp Brain Res* 126: 289–306, 1999. doi:10.1007/s002210050738.

Scholz JP, Schöner G. Use of the uncontrolled manifold (UCM) approach to understand motor variability, motor equivalence, and self-motion. In: *Progress in Motor Control: Skill Learning, Performance, Health, and Injury*, edited by Levin MF. New York: Springer, 2014, p. 91–100. doi:10.1007/978-1-4939-1338-1_7.

Scholz JP, Schöner G, Hsu WL, Jeka JJ, Horak F, Martin V. Motor equivalent control of the center of mass in response to support surface perturbations. *Exp Brain Res* 180: 163–179, 2007. doi:10.1007/s00221-006-0848-1.

Schoner G. Recent developments and problems in human movement science and their conceptual implications. *Ecol Psychol* 7: 291–314, 1995. doi:10.1207/s15326969eco0704_5.

Sherrington CS. *The Integrative Action of the Nervous System*. New Haven, CT: Yale University Press, 1906.

Shim JK, Olafsdottir H, Zatsiorsky VM, Latash ML. The emergence and disappearance of multi-digit synergies during force-production tasks. *Exp Brain Res* 164: 260–270, 2005. doi:10.1007/s00221-005-2248-3.

Shim JK, Park J, Zatsiorsky VM, Latash ML. Adjustments of prehension synergies in response to self-triggered and experimenter-triggered load and torque perturbations. *Exp Brain Res* 175: 641–653, 2006. doi:10.1007/s00221-006-0583-7.

Todorov E, Jordan MI. Optimal feedback control as a theory of motor coordination. *Nat Neurosci* 5: 1226–1235, 2002. doi:10.1038/nn963.

Togo S, Imamizu H. Anticipatory synergy adjustments reflect individual performance of feedforward force control. *Neurosci Lett* 632: 192–198, 2016. doi:10.1016/j.neulet.2016.08.032.

van Emmerik RE, van Wegen EE. On variability and stability in human movement. *J Appl Biomech* 16: 394–406, 2000. doi:10.1123/jab.16.4.394.

Wang Y, Asaka T, Zatsiorsky VM, Latash ML. Muscle synergies during voluntary body sway: combining across-trials and within-a-trial analyses. *Exp Brain Res* 174: 679–693, 2006. doi:10.1007/s00221-006-0513-8.

Wilhelm L, Zatsiorsky VM, Latash ML. Equifinality and its violations in a redundant system: multifinger accurate force production. *J Neurophysiol* 110: 1965–1973, 2013. doi:10.1152/jn.00461.2013.

Wolpert DM, Landy MS. Motor control is decision-making. *Curr Opin Neurobiol* 22: 996–1003, 2012. doi:10.1016/j.conb.2012.05.003.

Wu M, Matsubara JH, Gordon KE. General and specific strategies used to facilitate locomotor maneuvers. *PLoS One* 10: e0132707, 2015. doi:10.1371/journal.pone.0132707.

Zhou T, Wu YH, Bartsch A, Cuadra C, Zatsiorsky VM, Latash ML. Anticipatory synergy adjustments: preparing a quick action in an unknown direction. *Exp Brain Res* 226: 565–573, 2013. doi:10.1007/s00221-013-3469-5.